

## Mechanism of Two-Electron Oxidation of Deoxyguanosine 5'-Monophosphate by a Platinum(IV) Complex

Sunhee Choi,\*<sup>†</sup> Richard B. Cooley,<sup>†</sup> Amanda S. Hakemian,<sup>†</sup> Yuna C. Larrabee,<sup>†</sup>  
Richard C. Bunt,<sup>†</sup> Stéphane D. Maupas,<sup>‡</sup> James G. Muller,<sup>‡</sup> and  
Cynthia J. Burrows<sup>‡</sup>

*Contribution from the Department of Chemistry and Biochemistry, Middlebury College,  
Middlebury, Vermont 05753, and the Department of Chemistry, University of Utah,  
315 S. 1400 East, Salt Lake City, Utah 84112-0850*

Received September 4, 2003; E-mail: choi@middlebury.edu

**Abstract:** Many transition metal complexes mediate DNA oxidation in the presence of oxidizing radiation, photosensitizers, or oxidants. The final DNA oxidation products vary depending on the nature of metal complexes and the structure of DNA. Here we propose a mechanism of oxidation of a nucleotide, deoxyguanosine 5'-monophosphate (dGMP) by *trans*-*d,l*-1,2-diaminocyclohexanetetrachloroplatinum (*trans*-Pt(*d,l*)(1,2-(NH<sub>2</sub>)<sub>2</sub>C<sub>6</sub>H<sub>10</sub>)Cl<sub>4</sub>, [Pt<sup>IV</sup>Cl<sub>4</sub>(dach)]); dach = diaminocyclohexane) to produce 7,8-dihydro-8-oxo-2'-deoxyguanosine 5'-monophosphate (8-oxo-dGMP) stoichiometrically. The reaction was studied by high-performance liquid chromatography (HPLC), <sup>1</sup>H and <sup>31</sup>P nuclear magnetic resonance (NMR), and electrospray ionization mass spectrometry (ESI-MS). The proposed mechanism involves Pt<sup>IV</sup> binding to N7 of dGMP followed by cyclization via nucleophilic attack of a phosphate oxygen at C8 of dGMP. The next step is an inner-sphere, two-electron transfer to produce a cyclic phosphodiester intermediate, 8-hydroxyguanosine cyclic 5',8-(hydrogen phosphate). This intermediate slowly converts to 8-oxo-dGMP by reacting with solvent H<sub>2</sub>O.

### Introduction

Oxidative damage of DNA plays a critical role in mutagenesis, carcinogenesis, aging, and lethality.<sup>1</sup> DNA is oxidized by reactive oxygen species, ionizing radiation, and transition metal complexes. These oxidation reactions may induce modifications within the sugar or base moieties of DNA, leading to strand scission or base modification. Many transition metal complexes, including those of V, Cr, Mn, Re, Ru, Os, Co, Rh, Ni, Pd, and Cu, have been studied as potential probes of nucleic acid structure and for potential application as drugs.<sup>2</sup> They mediate DNA oxidation in the presence of oxidizing radiation, photosensitizers, or oxidants. Complexes including Cr<sup>VI</sup>, Mn<sup>II</sup>, Fe<sup>III</sup>, Co<sup>II</sup>, Ni<sup>II</sup>, and Cu<sup>II</sup> in the presence of O<sub>2</sub>, H<sub>2</sub>O<sub>2</sub>, or SO<sub>3</sub><sup>2-</sup> generate radicals that abstract one electron from guanine. Fe<sup>II</sup>-bleomycin, Fe<sup>II</sup>EDTA/H<sub>2</sub>O<sub>2</sub>, and photoinitiated charge-transfer complexes (Ru<sup>III</sup>) modify DNA by direct strand scission.<sup>2,3</sup> High-

valent oxometal (Mn<sup>V</sup>=O, Ru<sup>IV</sup>=O, Os<sup>IV</sup>=O, Cr<sup>V</sup>=O) complexes oxidize DNA at both sugar and base sites. The oxomanganese porphyrin, Mn-TMPyP/KHSO<sub>5</sub>, abstracts two electrons from guanine to produce the guanine cation, G<sup>+</sup>. The major oxidation product (>90%) from monomeric G is 2-amino-5-[(2-deoxy-β-D-erythro-pentofuranosyl)amino]-4H-imidazol-4-one (imidazolone), but several other oxidation products are formed from double-stranded oligonucleotides.<sup>4a,b</sup> Oxidation of a dinucleoside monophosphate d(GpT) by Mn<sup>V</sup>=O, proposed to be a two-electron mechanism, produces dehydroguanosinehydantoin as a major oxidation product.<sup>4c</sup> Ru<sup>III</sup> complexes coordinate to the N7 of deoxyguanosine<sup>5a</sup> and inosine<sup>5b</sup> and facilitate autooxidation of the nucleosides to yield the corresponding 8-ketonucleosides. Ru<sup>IV</sup>=O complexes oxidize guanine via an inner-sphere atom transfer to produce 7,8-dihydro-8-oxo-guanine (8-oxo-G).<sup>6</sup> High-valent nickel complexes (Ni<sup>III</sup>) formed from NiCR/KHSO<sub>5</sub> bind to N7 of G and react by a one-electron mechanism.<sup>7</sup> Cr<sup>V</sup>=O complexes initiate DNA cleavage through a Cr<sup>V</sup>-phosphate diester intermediate by hydrogen

<sup>†</sup> Middlebury College.

<sup>‡</sup> University of Utah.

- (1) (a) Sies, H. *Oxidative Stress: Oxidants and Antioxidants*; Academic Press: London, 1991. (b) Marnett, L. J.; Burcham, P. C. *Chem. Res. Toxicol.* **1993**, *6*, 771–785. (c) Cadet, J. In *DNA Adducts: Identification and Biological Significance*; Hemminki, K., Dipple, A., Shuker, D. G. E., Kadlubar, F. F., Segerbäck, D., Bartsch, H., Eds.; IARC Scientific Publication No. 125; Lyon, France, 1994; pp 245–276.
- (2) (a) Burrows, C. J.; Muller, J. G. *Chem. Rev.* **1998**, *98*, 1109–1151. (b) Pyle, A. M.; Barton, J. K. *Prog. Inorg. Chem.: Bioinorg. Chem.* **1990**, *38*, 413–475. (c) Chow, C. S.; Barton, J. K. *Methods Enzymol.* **1992**, *212*, 219–242.
- (3) (a) Stubbe, J.; Kozarich, J. W. *Chem. Rev.* **1987**, *87*, 1107–1136. (b) Pogozelski, W. K.; McNeese, T. J.; Tullius, T. D. *J. Am. Chem. Soc.* **1995**, *117*, 6428–6433. (c) Yang, I. V.; Thorp, H. H. *Inorg. Chem.* **2000**, *39*, 4969–4976.

- (4) (a) Vialas, C.; Pratviel, G.; Claparols, C.; Meunier, B. *J. Am. Chem. Soc.* **1998**, *120*, 11548–11553. (b) Vialas, C.; Claparols, C.; Pratviel, G.; Meunier, B. *J. Am. Chem. Soc.* **2000**, *122*, 2157–2167. (c) Chworos, A. C.; Coppel, Y.; Dubey, I.; Pratviel, G.; Meunier, B. *J. Am. Chem. Soc.* **2001**, *123*, 5867–5877.
- (5) (a) Clarke, M. J.; Morrissey, P. E. *Inorg. Chim. Acta* **1984**, *80*, L69–70. (b) Gariepy, K. C.; Curtin, M. A.; Clarke, M. J. *J. Am. Chem. Soc.* **1989**, *111*, 4947–4952.
- (6) (a) Farrer, B. T.; Thorp, H. H. *Inorg. Chem.* **2000**, *39*, 44–49. (b) Carter, P. J.; Cheng, C.-C.; Thorp, H. H. *J. Am. Chem. Soc.* **1998**, *120*, 632–642. (c) Carter, C. P.; Cheng, C.-C.; Thorp, H. H. *Inorg. Chem.* **1996**, *35*, 3348–3354. (d) Cheng, C.-C.; Goll, J. G.; Neyhart, G. A.; Welch, T. W.; Singh, P.; Thorp, H. H. *J. Am. Chem. Soc.* **1995**, *117*, 2970–2980.

abstraction from C1'.<sup>8</sup> Some transition metals such as Ir<sup>IV</sup>, MnO<sub>4</sub><sup>2-</sup>, Os<sup>III</sup>, and Ru<sup>III</sup> are reported to further oxidize 8-oxo-G,<sup>9</sup> a major oxidation product of guanine in double-stranded DNA.<sup>2</sup>

Platinum coordination complexes are biologically important for their anticancer activities.<sup>10</sup> Pt<sup>II</sup> complexes bind preferentially to the N7 position of G.<sup>11</sup> Cisplatin, *cis*-diamminedichloroplatinum(II), binds bifunctionally to adjacent Gs and kinks DNA.<sup>11b</sup> High mobility group proteins and p53 protein bind to the platinum-modified DNA, preventing DNA replication, and leading to cell death.<sup>11c</sup> Some Pt<sup>IV</sup> complexes have shown potential as powerful anticancer drugs, although most Pt<sup>IV</sup> anticancer drugs have been considered to be Pt<sup>II</sup> prodrugs.<sup>12</sup> Because Pt<sup>IV</sup> complexes are kinetically inert,<sup>13</sup> reaction with DNA is not expected until they have been reduced to Pt<sup>II</sup> in the cellular medium.<sup>12</sup> However, direct Pt<sup>IV</sup> binding to DNA has been observed in vitro in several labs.<sup>14–16</sup> Choi et al. reported that Pt<sup>IV</sup> complexes with highly electron-withdrawing and bulky ligands have high reduction potentials<sup>15a</sup> and high reactivity toward the monomeric nucleotide GMP.<sup>15b</sup> Furthermore, [Pt<sup>IV</sup>-Cl<sub>4</sub>(dach)], which has a high reduction potential, oxidizes guanine in GMP, dGMP, 2'-deoxyguanosine (dG), 2'-deoxyguanylyl-(3'→5')-2'-deoxyguanosine [d(GpG)], and a double-stranded oligonucleotide without any UV radiation or additional

oxidants.<sup>15c</sup> The major oxidation product was identified as 8-oxo-G. We also observed that [Pt<sup>IV</sup>Cl<sub>4</sub>(dach)] further oxidizes 8-oxo-G.

It is important to study the mechanism in detail because the redox reaction between DNA and Pt<sup>IV</sup> complexes represents new chemistry. In this paper, we propose a detailed mechanism of the redox reaction between [Pt<sup>IV</sup>Cl<sub>4</sub>(dach)] and dGMP based on UV-visible, HPLC, <sup>1</sup>H and <sup>31</sup>P NMR, and ESI-MS studies. The mechanism involves Pt<sup>IV</sup> binding to N7 of dGMP followed by cyclization of a phosphate oxygen to C8 of dGMP. This study provides the most detailed insight to date of the mechanism of two-electron oxidation of guanine by a transition metal complex and provides structural characterization of a new cyclic nucleotide as the initial product.

## Results

**Identification of a Pt<sup>IV</sup>-dGMP Intermediate, I.** The time course of the reaction of [Pt<sup>IV</sup>Cl<sub>4</sub>(dach)]/dGMP (10 mM/20 mM) was monitored by <sup>1</sup>H NMR spectroscopy, and results paralleled those previously obtained with GMP.<sup>15b</sup> Figure 1a shows the <sup>1</sup>H NMR spectra in the 9 ppm region. The multiplet peak at 9.3 ppm is assigned to H8 of Pt<sup>IV</sup> bound to N7 of dGMP.<sup>15b,16</sup> The concentration of Pt<sup>IV</sup>-dGMP at various reaction times was calculated by multiplying 20 mM by the area under the 9.3 ppm peak relative to that at 8.3 ppm (H8 of free dGMP) at *t* = 0, and these are displayed in Figure 2 as a function of time. The concentration reaches a maximum at 4 h and gradually decreases, indicating that the Pt<sup>IV</sup>-dGMP adduct is an intermediate.

Intermediate **I** was also detected by HPLC (Figure 3). The HPLC chromatogram of the reaction at *t* = 0 shows two peaks with retention times of 4.6 and 6.2 min due to free dGMP and free [Pt<sup>IV</sup>Cl<sub>4</sub>(dach)], respectively. After a 1-h reaction time (data not shown), the [Pt<sup>IV</sup>Cl<sub>4</sub>(dach)]/dGMP (10 mM/20 mM) solution shows a new set of peaks with a retention time of 10.9 min. The UV/visible spectrum of this peak obtained directly from the HPLC diode-array detector (DAD) is different from that of free dGMP (Figure 4). It has a large UV absorption below 220 nm due to Pt<sup>IV</sup> and a  $\lambda_{\text{max}}$  of 252 nm with a shoulder at 280 nm. In contrast, free dGMP has no absorption below 220 nm and a  $\lambda_{\text{max}}$  of 254 nm with a shoulder at 272 nm. The intensity of this 10.9 min peak reaches a maximum around 4 h (Figure 3) and falls off afterward, which is the same trend as the peak at 9.2 ppm in <sup>1</sup>H NMR spectra (Figure 2). The UV absorption feature along with the <sup>1</sup>H NMR data support the proposal that **I** is the Pt<sup>IV</sup>-dGMP adduct.

**Identification of a Guanosine-Cyclic Phosphodiester, II.** Figure 1b displays the time course of the reaction of [Pt<sup>IV</sup>Cl<sub>4</sub>(dach)]/dGMP (10 mM/20 mM) in the 6 ppm region. The peak at 6.46 ppm is assigned to H1' of free dGMP. There are three new peaks in this area upon reaction with Pt<sup>IV</sup>. The peak centered at 6.57 ppm grows in intensity, reaches a maximum, and gradually diminishes. The peaks at 6.36 and 6.42 ppm are assigned to the H1' of the final products, 8-oxo-dGMP and the Pt<sup>II</sup>-dGMP adduct, respectively. The assignment was made by comparing the H1' region of <sup>1</sup>H NMR spectra of authentic 8-oxo-dGMP (6.36 ppm) and [Pt<sup>II</sup>Cl(dach)(dGMP)] (6.42 ppm). The concentrations of the species giving the peak at 6.57 ppm at various reaction times were calculated by multiplying 20 mM

- (7) (a) Muller, J. G.; Kayser, L. A.; Paikoff, S. J.; Duarte, V.; Tang, N.; Perez, R. J.; Rokita, S. E.; Burrows, C. J. *Coord. Chem. Rev.* **1999**, *185–186*, 761–774. (b) Burrows, C. J.; Perez, R. J.; Muller, J. G.; Rokita, S. E. *Pure Appl. Chem.* **1998**, *70*, 275–278. (c) Muller, J. G.; Chen, X.; Dadiz, A. C.; Rokita, S. E.; Burrows, C. J. *J. Am. Chem. Soc.* **1992**, *114*, 6407–6411.
- (8) (a) Bose, R. N.; Moghaddas, S.; Mazzer, P. A.; Dudones, L. P.; Joudah, L.; Stroup, D. *Nucleic Acids Res.* **1999**, *27*, 2219–2226. (b) Bose, R. N.; Fonkeng, B. S. *Chem. Commun.* **1996**, 2211–2212. (c) Bose, R. N.; Fonkeng, B. S.; Moghaddas, S.; Stroup, D. *Nucleic Acids Res.* **1998**, *26*, 1588–1596. (d) Sugden, K. D.; Wetterhahn, K. E. *Chem. Res. Toxicol.* **1997**, *10*, 1397–1406.
- (9) (a) Muller, J. G.; Duarte, V.; Hickerson, R. P.; Burrows, C. J. *Nucleic Acids Res.* **1998**, *26*, 2247–2249. (b) Koizume, S.; Inoue, H.; Kamiya, H.; Ohtsuka, E. *Nucleic Acids Res.* **1998**, *26*, 3599–3607. (c) Sarala, R.; Islam, A. M.; Rabin, S. B.; Stanburg, D. M. *Inorg. Chem.* **1990**, *29*, 1133–1142. (d) Ropp, P. A.; Thorp, H. H. *Chem. Biol.* **1999**, *6*, 599–605. (e) Luo, W.; Muller, J. G.; Rachlin, E. M.; Burrows, C. J. *Org. Lett.* **2000**, *2*, 613–616.
- (10) (a) Lippert, B. *Cisplatin: Chemistry and Biochemistry of a Leading Anticancer Drug*; Wiley-VCH: Weinheim, Germany, 1999. (b) Howell, S. B. *Platinum and Other Metal Coordination Compounds in Cancer Chemotherapy*; Plenum: New York, 1991.
- (11) (a) Reedijk, J. *Chem. Commun.* **1996**, 801–806. (b) Takahara, P. M.; Rosenzweig, A. C.; Frederick, C. A.; Lippard, S. J. *Nature* **1995**, *377*, 649–651. (c) Ohndorf, U.-M.; Rould, M. A.; He Q.; Pabo, C. O.; Lippard, S. J. *Nature* **1999**, *399*, 708–712.
- (12) (a) Hall, M. D.; Hambley, T. W. *Coord. Chem. Rev.* **2002**, *232*, 49–67. (b) Eastman, A. *Biochem. Pharmacol.* **1987**, *36*, 4177–4178. (c) Chaney, S. G. *Int. J. Oncol.* **1995**, *6*, 1291–1305. (d) Chaney, S. G.; Gibbons, G. R.; Wyrick, S. D.; Podhasky, P. *Cancer Res.* **1991**, *51*, 969–973. (e) Kelland, L. R.; Murrer, B. A.; Abel, G.; Giandomenico, C. M.; Mistry, P.; Harrap, K. R. *Cancer Res.* **1992**, *52*, 822–828. (f) Oshita, F.; Eastman, A. *Oncol. Res.* **1993**, *5*, 111–118. (g) Yoshida, M.; Khokhar, A. R.; Zhang, Y.-P.; Siddik, Z. H. *Cancer Res.* **1994**, *54*, 4691–4697.
- (13) (a) Hartley, F. R. *Chemistry of the Platinum Group Metals: Recent Developments*; Elsevier: Amsterdam, 1991. (b) Basolo, F.; Pearson, R. G. *Mechanism of Inorganic Reactions*; Wiley: New York, 1967.
- (14) (a) Novakova, O.; Vrana, O.; Kiseleva, V. I.; Brabec, V. *Eur. J. Biochem.* **1995**, *228*, 616–624. (b) Talman, E. G.; Kidani, Y.; Mohrmann, L.; Reedijk, J. *Inorg. Chim. Acta* **1998**, *283*, 251–255. (c) Galanski, M.; Keppler, B. K. *Inorg. Chim. Acta* **2000**, *300*, 300–302, 783–789.
- (15) (a) Choi, S.; Filotto, C.; Bisanzo, M.; Delaney, S.; Lagasee, D.; Whitworth, J. L.; Jusko, A.; Li, C.; Wood, N. A.; Willingham, J.; Schwenker, A.; Spaulding, K. *Inorg. Chem.* **1998**, *37*, 2500–2504. (b) Choi, S.; Mahalingaiah, S.; Delaney, S.; Neale, N. R.; Masood, S. *Inorg. Chem.* **1999**, *38*, 1800–1805. (c) Choi, S.; Orbai, L.; Padgett, E. J.; Delaney, S.; Hakemian, A. S. *Inorg. Chem.* **2001**, *40*, 5481–5482.
- (16) (a) Roat, R. M.; Reedijk, J. *J. Inorg. Biochem.* **1993**, *52*, 263–274. (b) Talman, E. G.; Brüning, W.; Reedijk, J.; Spek, A. L.; Veldman, N. *Inorg. Chem.* **1997**, *36*, 854–861. (c) van der Veer, J. L.; Peters, A. R.; Reedijk, J. *J. Inorg. Biochem.* **1986**, *26*, 137–142. (d) Roat, R. M.; Jerardi, M. J.; Kopy, C. B.; Heath, D. C.; Clark, J. A.; DeMars, J. A.; Weaver, J. M.; Bezemer, E.; Reedijk, J. *J. Chem. Soc., Dalton Trans.* **1997**, 3615–3621.

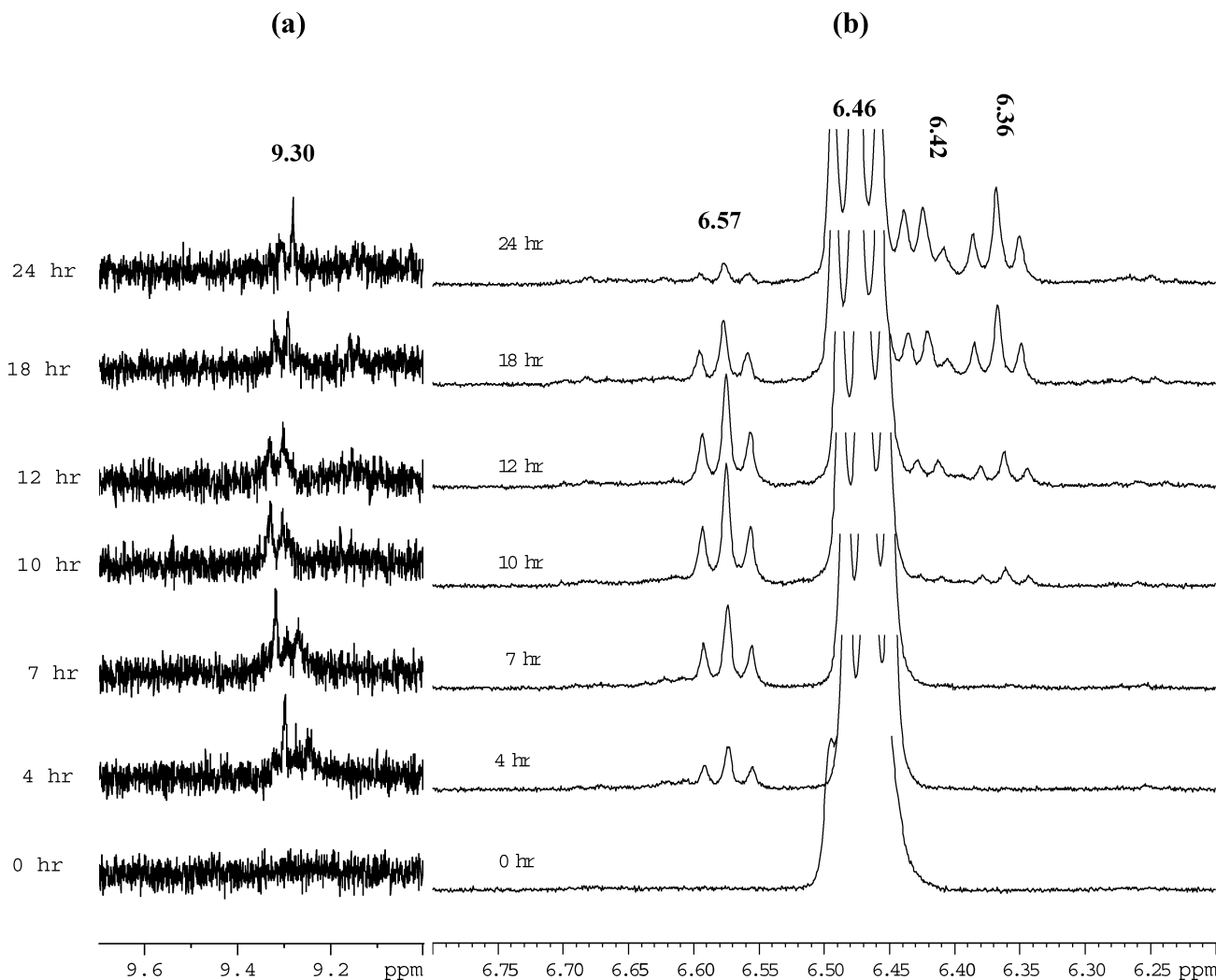


**Figure 1.** Time-dependent  $^1\text{H}$  NMR spectra of the reaction of 10 mM  $[\text{Pt}^{\text{IV}}\text{Cl}_4(\text{dach})]$  with 20 mM dGMP at pH 8.6 ( $t = 0$ ) and  $37^\circ\text{C}$ .

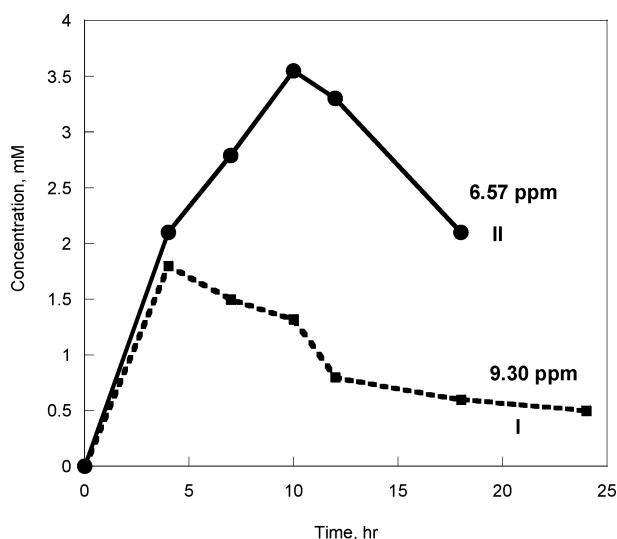


**Figure 2.** Time-dependent concentrations of **I** and **II** generated from the reaction of 10 mM  $[\text{Pt}^{\text{IV}}\text{Cl}_4(\text{dach})]$  with 20 mM dGMP at pH 8.6 ( $t = 0$ ) and  $37^\circ\text{C}$ . They were calculated from the  $^1\text{H}$  NMR peaks at 9.30 and 6.57 ppm, respectively.

by the area of the peak relative to that of 6.46 ppm at  $t = 0$ . These are overlaid with the concentration of **I** in Figure 2. The intermediate giving the 6.57 ppm peak reaches a maximum

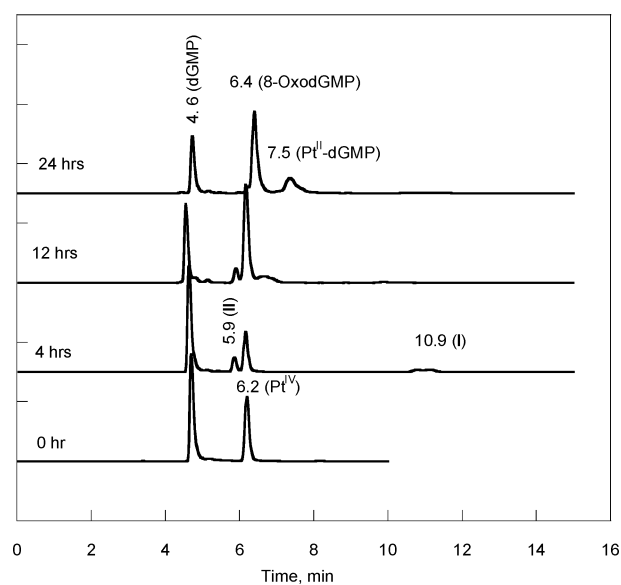


**Figure 3.** Reversed-phase HPLC chromatograms (DAD,  $\lambda = 294\text{ nm}$ ) of the reaction of 10 mM  $[\text{Pt}^{\text{IV}}\text{Cl}_4(\text{dach})]$  with 20 mM dGMP at pH 8.6 ( $t = 0$ ) and  $37^\circ\text{C}$ .

concentration of 3.5 mM after 10 h, while **I** reaches a maximum concentration of 1.9 mM after 4 h. Therefore we conclude that there is a second intermediate.

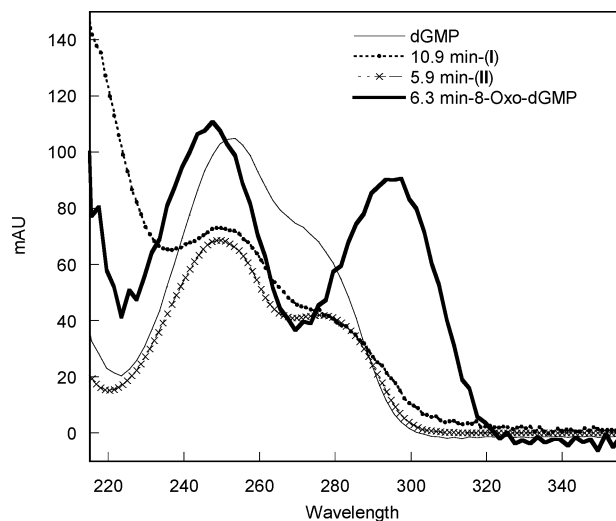


**Figure 4.** UV spectra of dGMP, **I**, **II**, and 8-oxo-dGMP obtained directly from the diode array detector of the HPLC. The retention times of the intermediate correspond to the chromatograms in Figure 3.

Intermediate **II** was also detected by HPLC. A new peak with a retention time of 5.9 min is seen in the  $t = 4$  and 12 h reaction chromatograms in Figure 3. The UV/visible spectrum of this peak obtained directly from the HPLC DAD has a  $\lambda_{\text{max}}$  at 252 and 280 nm and is different from those of free dGMP and **I** (Figure 4). The intensity of the 5.9 min peak reaches a maximum around 10 h and falls off afterward, which is the same trend as the peak at 6.57 ppm in the  $^1\text{H}$  NMR spectra (Figure 2).

A fraction containing **II** was collected directly from HPLC runs of 10-h reaction mixtures and analyzed by negative ion ESI-MS. The molecular ion of **II** occurs at  $m/z$  344, which is 2 units lower than that of dGMP. The  $m/z$  of **II** was unchanged in a reaction conducted in 95%  $\text{H}_2^{18}\text{O}$  vs  $\text{H}_2^{16}\text{O}$  (vide infra).

The  $^{31}\text{P}$  NMR spectra of the reaction mixture at various times indicate the phosphorus atom in **II** is in a different environment than in dGMP (Figure 5). The peak at 5.0 ppm at  $t = 0$  arises from  $^{31}\text{P}$  of free dGMP. It gradually shifts upfield as the reaction progresses, eventually appearing at 2.5 ppm at  $t = 16$  h. Usually orthophosphate and nucleoside 5'- and 3'-phosphates appear in this chemical shift region,<sup>18</sup> but this upfield shift is likely due to the lowering of the pH as the reaction proceeds. The pH of the reaction was adjusted to 8.6 at  $t = 0$ . It gradually drops to pH 4.0 at  $t = 16$  h (Figure 6), which is due to the production of two protons in the two-electron redox reaction (vide infra).

It is known that both inorganic and nucleotide phosphates shift upfield at lower pH.<sup>8c,18a</sup> The peak at 2.95 ppm on the shoulder of the 2.5 ppm peak on the  $t = 16$  h spectrum is due to 8-oxo-dGMP, which was confirmed by the  $^{31}\text{P}$  NMR spectrum of authentic 8-oxo-dGMP. At  $t = 2$  h (data not shown), a new peak at  $-5.5$  ppm appears. It grows in intensity, reaches a maximum, and gradually diminishes as the reaction progresses. We believe that this peak is due to **II**. The resonance position of this peak does not change at different reaction times, indicating that it is pH-insensitive. It is known that the  $^{31}\text{P}$  NMR peak of cyclic phosphodiester appears upfield relative to that of phosphate and is pH-insensitive.<sup>18a</sup> For example, the  $^{31}\text{P}$  NMR

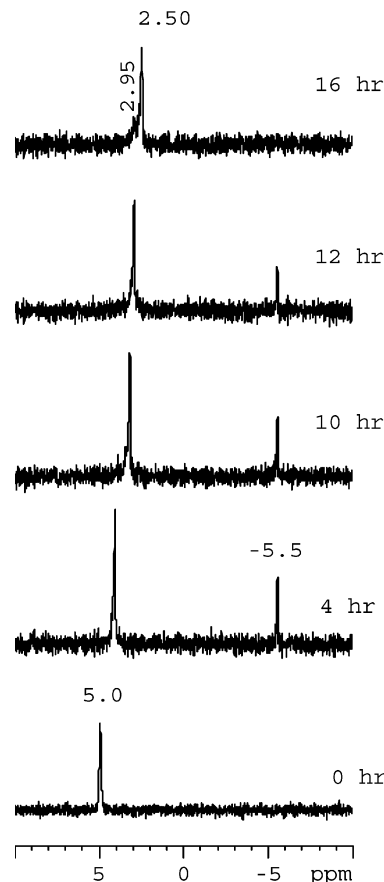


**Figure 5.** Time-dependent  $^{31}\text{P}$  NMR spectra of the reaction of 10 mM  $[\text{Pt}^{\text{IV}}\text{Cl}_4(\text{dach})]$  with 20 mM dGMP at pH 8.6 ( $t = 0$ ) and 37 °C.

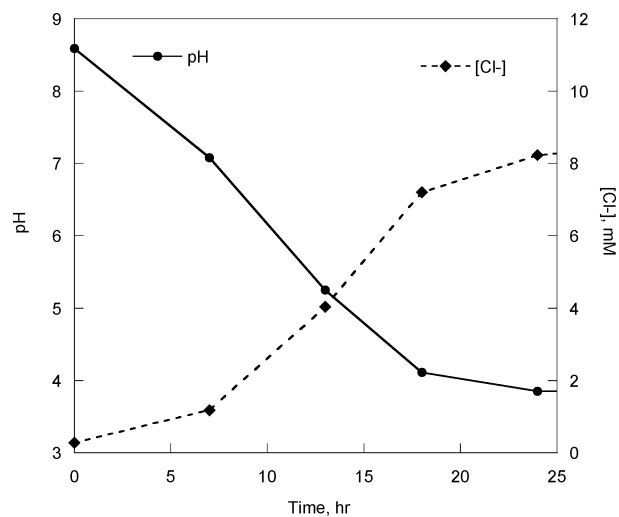


**Figure 6.** pH and  $[\text{Cl}^-]$  vs time for the reaction of 5 mM  $[\text{Pt}^{\text{IV}}\text{Cl}_4(\text{dach})]$  with 5 mM dGMP at pH 8.6 ( $t = 0$ ) and 37 °C.

peak of 3',5'-cyclicAMP appears at  $-1$  ppm compared to 2 ppm in AMP, and it is pH-insensitive.

Therefore, on the basis of UV, ESI-MS, and  $^{31}\text{P}$  NMR, we propose that the intermediate **II** is 8-hydroxyguanosine cyclic 5',8-(hydrogen phosphate). It has the characteristic UV and  $^{31}\text{P}$  NMR spectra of 5',8-cyclo-guanosine<sup>17</sup> and two fewer hydrogens (2 amu) than dGMP.

#### Identification of the Final Oxidation Product of dGMP.

The HPLC fraction containing the 6.2 min (Figure 3) or 9 min (Figure 7) peak was collected. Its UV spectrum shows  $\lambda_{\text{max}}$  at

(17) Guengerich, F. P.; Mundkowski, R. G.; Voehler, M.; Kadlubar, F. F. *Chem. Res. Toxicol.* **1999**, *12*, 906–916.

(18) (a) Robitaille, P.-M. L.; Robitaille, P. A.; Brown, G. G., Jr.; Brown, G. G. *J. Magn. Reson.* **1991**, *92*, 73–84. (b) Dennis, A. L.; Puskas, M.; Stasaitis, S.; Sandwick, R. K. *J. Inorg. Biochem.* **2000**, *81*, 73–80.



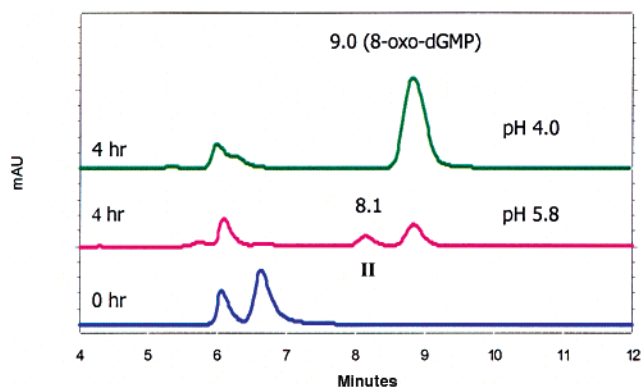


**Figure 7.** HPLC chromatograms (DAD  $\lambda = 280$  nm) of the reaction of 10 mM  $[\text{Pt}^{\text{IV}}\text{Cl}_4(\text{dach})]$  with 20 mM dGMP at pH 8.6 ( $t = 0$ ) and 37 °C.

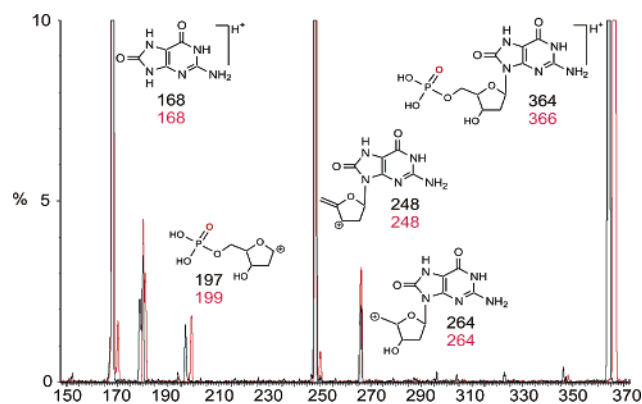


**Figure 8.** Positive-ion ESI-MS/MS analysis of fragment ions of 8-oxo-dGMP produced from the reaction of 10 mM  $[\text{Pt}^{\text{IV}}\text{Cl}_4(\text{dach})]$  with 20 mM dGMP at pH 8.6 ( $t = 0$ ) and 37 °C after 12 h. Black, reaction conducted in  $\text{H}_2^{16}\text{O}$ ; red, reaction conducted in  $\text{H}_2^{18}\text{O}$ .

247 and 290 nm (Figure 4), coinciding with the literature values for 8-oxo-G.<sup>19</sup>

Fragmentation with positive-ion ESI-MS/MS displayed an  $m/z = 364$  (Figure 8), the same  $m/z$  as 8-oxo-dGMP that is 16 units higher than dGMP ( $m/z$  348). Furthermore, the  $^1\text{H}$  (6.37 ppm) and  $^{31}\text{P}$  NMR (3.0 ppm) spectra of this fraction were exactly the same as those of authentic 8-oxo-dGMP. Therefore, we conclude that the final oxidation product of dGMP is 8-oxo-dGMP.

**Origin and Location of the Added Oxygen in 8-Oxo-dGMP.** Experiments conducted under nitrogen in the absence of  $\text{O}_2$  also produced 8-oxo-dGMP. When 95%  $\text{H}_2^{18}\text{O}$  was used as solvent, the molecular ion of 8-oxo-dGMP was 2 amu higher (366 amu) than that from the reaction in  $\text{H}_2^{16}\text{O}$  (Figure 8). This indicates that the origin of the oxygen atom gained in the formation of 8-oxo-dGMP is solvent water.

The location of the added oxygen from water could be deduced by comparing the positive-ion ESI-MS/MS of the fragments of 8-oxo-dGMP from the reaction in  $\text{H}_2^{18}\text{O}$  to those in  $\text{H}_2^{16}\text{O}$ . Only 1% of the fragments of  $m/z = 168$  (assigned as 7,8-dihydro-8-oxoguanine from cleavage of the glycosidic bond) and  $m/z = 248$  (due to 7,8-dihydro-8-oxoguanosine) change mass as a function of isotopically labeled solvent, indicating that for the bulk of the material neither the base nor ribose contains the oxygen atom derived from water. The fragment at  $m/z = 197$  is assigned as the phosphate–ribose moiety, and it

shifted to 199 when the reaction was conducted in  $\text{H}_2^{18}\text{O}$ . Therefore, we conclude that the new oxygen atom gained from water resides on the phosphate group of 8-oxo-dGMP. However, a minor pathway ( $\leq 1\%$ ) involves direct incorporation of  $^{18}\text{O}$  into 8-oxo-dGMP from solvent.

**Identification of  $[\text{Pt}^{\text{II}}\text{Cl}_2(\text{dach})]$  and  $[\text{Pt}^{\text{II}}\text{Cl}(\text{dach})(\text{dGMP})]$ .** The final reduction products of  $[\text{Pt}^{\text{IV}}\text{Cl}_4(\text{dach})]$  consist of  $[\text{Pt}^{\text{II}}\text{Cl}_2(\text{dach})]$  and  $[\text{Pt}^{\text{II}}\text{Cl}(\text{dach})(\text{dGMP})]$ . Since the solubility of  $[\text{Pt}^{\text{II}}\text{Cl}_2(\text{dach})]$  is very low ( $\sim 1$  mM), most of the  $[\text{Pt}^{\text{II}}\text{Cl}_2(\text{dach})]$  precipitates as orange crystals. The FTIR spectrum of the orange crystals is identical to that of an authentic sample of  $[\text{Pt}^{\text{II}}\text{Cl}_2(\text{dach})]$ .<sup>15c</sup> The existence of  $[\text{Pt}^{\text{II}}\text{Cl}(\text{dach})(\text{dGMP})]$  in solution was shown by  $^1\text{H}$  NMR and HPLC. The  $^1\text{H}$  NMR spectra of the regions around 8, 6, and 2 ppm of the final reaction mixture display the same peaks at 8.65, 6.42, and 2.23 ppm as authentic  $[\text{Pt}^{\text{II}}\text{Cl}(\text{dach})(\text{dGMP})]$ . The peaks at 8.65 and 2.23 ppm (Figure 9) are due to H8 of dGMP and H1 of dach bound to  $\text{Pt}^{\text{II}}$ , respectively. The peak at 6.42 ppm (Figure 1b) is due to H1' of  $\text{Pt}^{\text{II}}$ –dGMP adduct. The HPLC chromatogram (Figure 3) of the reaction mixture of  $[\text{Pt}^{\text{IV}}\text{Cl}_4(\text{dach})]/\text{dGMP}$  (10 mM/20 mM) at  $t = 24$  h shows the peak at 7.5 min that is due to  $[\text{Pt}^{\text{II}}\text{Cl}(\text{dach})-(\text{dGMP})]$ .

**Stoichiometry of the Reaction.** Figure 6 displays the pH and the concentration of chloride for the reaction of  $[\text{Pt}^{\text{IV}}\text{Cl}_4(\text{dach})]$  with dGMP (both 5 mM) as a function of time. It clearly shows the production of both  $\text{H}^+$  and  $\text{Cl}^-$  during the course of the reaction. The concentration of dGMP at various time intervals was obtained by comparison of calibration curves of authentic dGMP with HPLC chromatograms obtained with DAD monitoring at 280 nm. Because of the hydrolysis of  $[\text{Pt}^{\text{IV}}\text{Cl}_4(\text{dach})]$ , it was difficult to quantify  $[\text{Pt}^{\text{IV}}\text{Cl}_4(\text{dach})]$  by HPLC. However, the chemical shifts of the  $^1\text{H}$  NMR peaks (3.31, 2.42, 1.82, and 1.43 ppm) of aqueous  $[\text{Pt}^{\text{IV}}\text{Cl}_4(\text{dach})]$  stay the same over several days. Since the peak at 2.42 ppm was sensitive to the oxidation state of platinum [2.42 ppm for  $\text{Pt}^{\text{IV}}$  and 2.23 ppm for  $\text{Pt}^{\text{II}}$  (Figure 9)], we used the relative intensity of this peak compared to the internal standard, 3-(trimethylsilyl)propionic acid, to calculate the concentration of the unreacted  $[\text{Pt}^{\text{IV}}\text{Cl}_4(\text{dach})]$ . The concentration of 8-oxo-dGMP was obtained by comparison of a calibration curve of authentic 8-oxo-dGMP with HPLC chromatograms obtained with DAD at 280 nm. (Figure 7). To obtain the overall total concentration of 8-oxo-dGMP generated from the reactants, the solution was acidified to pH 4 in order to quickly convert all of **II** to 8-oxo-dGMP. When the 4 h reaction mixture at pH 5.8 was analyzed immediately by HPLC, **II** appeared at 8.1 min and then disappeared in the acidified solution (pH 4.0) (Figure 7). The intensity of the 9.0 min peak in the pH 4.0 solution increases compared to that of the pH 5.8 solution, confirming that all of **II** was converted to 8-oxo-dGMP. We obtained the total concentration of 8-oxo-dGMP from the intensity of the 9.0 min peak of the acidified solution. The concentrations of reacted dGMP,  $[\text{Pt}^{\text{IV}}\text{Cl}_4(\text{dach})]$ , and total 8-oxo-dGMP are displayed in Figure 10.

The concentration of reacted dGMP and  $[\text{Pt}^{\text{IV}}\text{Cl}_4(\text{dach})]$  are the same within experimental error, indicating that 1 equiv of dGMP reacts with 1 equiv of  $[\text{Pt}^{\text{IV}}\text{Cl}_4(\text{dach})]$ . The concentration–time profile of 8-oxo-dGMP is symmetrical to those of reactants, indicating that 1 equiv of  $[\text{Pt}^{\text{IV}}\text{Cl}_4(\text{dach})]$  converts 1 equiv of dGMP to 1 equiv of 8-oxo-dGMP. For the 10-h reaction mixture of 10 mM  $[\text{Pt}^{\text{IV}}\text{Cl}_4(\text{dach})]$  and 20 mM dGMP (pH 8.6

(19) Culp, S. J.; Cho, B. P.; Kadlubar, F. F.; Evans, F. E. *Chem. Res. Toxicol.* **1989**, *2*, 416–422.

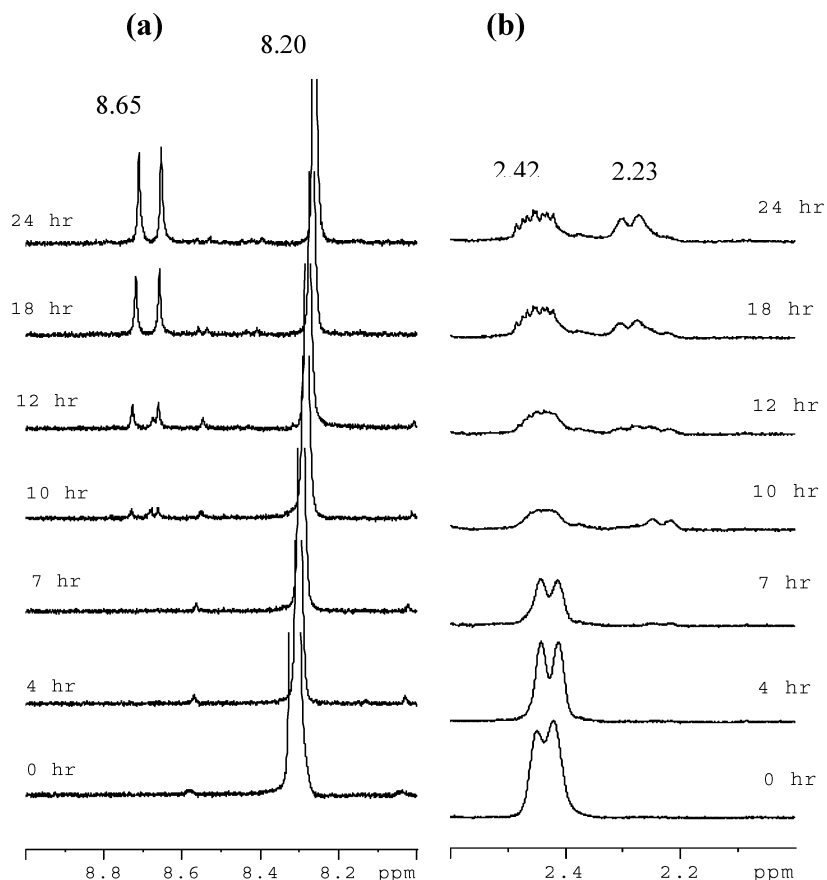


**Figure 9.** Time-dependent  $^1\text{H}$  NMR spectra of the reaction of 10 mM  $[\text{Pt}^{\text{IV}}\text{Cl}_4(\text{dach})]$  with 20 mM dGMP at pH 8.6 ( $t = 0$ ) and  $37^\circ\text{C}$ .

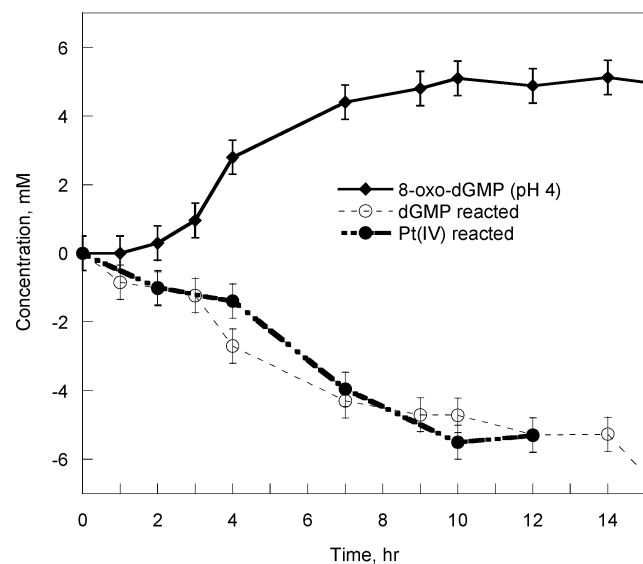
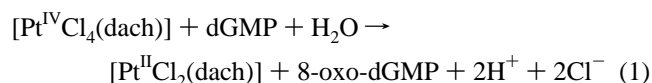


**Figure 10.** Time-dependent concentrations of  $\text{Pt}^{\text{IV}}(\text{dach})\text{Cl}_4$  and dGMP consumed and total 8-oxo-dGMP produced from the reaction of 10 mM  $\text{Pt}^{\text{IV}}(\text{dach})\text{Cl}_4$  with 20 mM dGMP at pH 8.6 ( $t = 0$ ) and  $37^\circ\text{C}$ .

at  $t = 0$ ), approximately 5 mM  $[\text{Pt}^{\text{IV}}\text{Cl}_4(\text{dach})]$  and dGMP were consumed to produce 5 mM 8-oxo-dGMP. Therefore, the overall reaction can be written as



For the reaction of equimolar  $[\text{Pt}^{\text{IV}}\text{Cl}_4(\text{dach})]$  and dGMP (10 mM), a small amount ( $\sim 5\%$  relative to 8-oxo-dGMP) of

guanidinohydantoin was observed by negative-ion LC-ESI-MS ( $m/z = 352$ , or  $+6$  relative to dGMP) after 20 h. Guanidinohydantoin is a further oxidation product of 8-oxo-dGMP by  $[\text{Pt}^{\text{IV}}\text{Cl}_4(\text{dach})]$ .

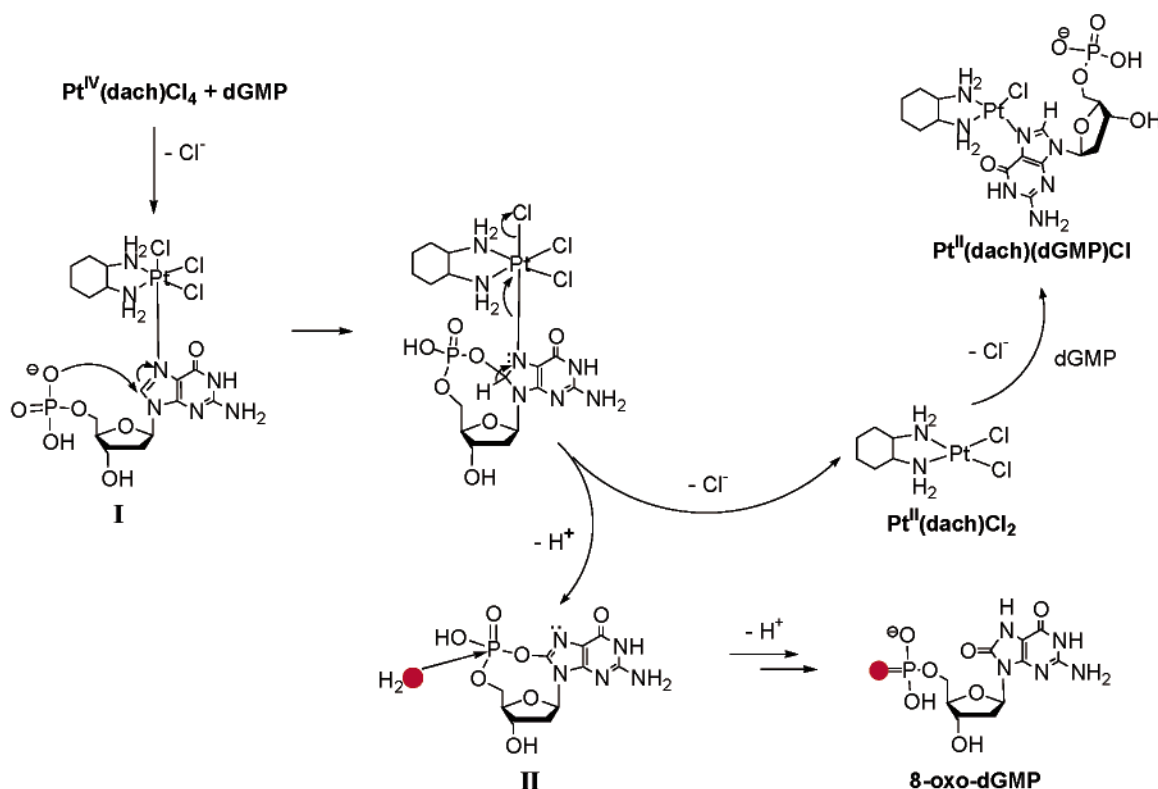
## Discussion

According to eq 1, the overall reaction generates two protons, one 8-oxo-dGMP, and two chlorides when one  $\text{Pt}^{\text{IV}}$  and one dGMP are allowed to react. To our knowledge, the present study reports the only system in which 8-oxo-G is generated cleanly and stoichiometrically from the transition metal oxidation of a mononucleotide. One-electron photooxidation of the dG nucleoside generates imidazolone and its hydrolysis product oxazolone as major products.<sup>20</sup> Two-electron oxidation of  $\text{dG}^{4a,b}$  and the dinucleotide  $\text{d}(\text{GpT})^{4c}$  by  $\text{Mn}^{\text{V}}=\text{O}$  produces imidazolone and dehydroguanidinohydantoin, respectively. Although it is reported that  $\text{Ru}^{\text{IV}}=\text{O}$  complexes oxidize guanine via an inner-sphere, oxygen atom transfer to produce 8-oxo-G,<sup>6</sup> the detailed mechanism and stoichiometry have not been reported.

The HPLC, UV–visible,  $^1\text{H}$  and  $^{31}\text{P}$  NMR, and ESI-MS studies lead us to propose the mechanism in Scheme 1. The first step is loss of  $\text{Cl}^-$  from  $[\text{Pt}^{\text{IV}}\text{Cl}_4(\text{dach})]$ , followed by binding to G N7. In a previous study,<sup>15b</sup> we reported that the decay of  $[\text{Pt}^{\text{IV}}\text{Cl}_4(\text{dach})]$  is sigmoidal in shape, indicating that the reaction is autocatalyzed. Although we show the axial chloride substituted with dGMP, it is also possible that the equatorial chloride

(20) (a) Raoul, S.; Berger, M.; Buchko, G. W.; Joshi, P. C.; Morin, B.; Weinfeld, M.; Cadet, J. *J. Chem. Soc., Perkin Trans. 2* **1996**, 371–381. (b) Gasparutto, D.; Ravanat, J.-L.; Gerot, O.; Cadet, J. *J. Am. Chem. Soc.* **1998**, *120*, 10283–10286.

Scheme 1. Proposed Mechanism



could be replaced. The next step involves nucleophilic attack at C8 by an oxygen anion of the phosphate group, producing a cyclic phosphodiester. The next step is an inner-sphere, two-electron transfer from bound dGMP to  $\text{Pt}^{\text{IV}}$ . At this point, the H8 proton and one more chloride are released to form the 8-hydroxyguanosine 5',8 cyclic phosphodiester and  $[\text{Pt}^{\text{II}}\text{Cl}_2(\text{dach})]$ . The cyclic phosphodiester slowly hydrolyzes to form 8-oxo-dGMP, a process that is faster at lower pH. Indeed, higher quantities of intermediate **II**, now assigned as the cyclic phosphodiester, could be isolated by HPLC if the pH was kept at 7 or above. The  $[\text{Pt}^{\text{II}}\text{Cl}_2(\text{dach})]$  produced can also bind to another dGMP to form  $[\text{Pt}^{\text{II}}\text{Cl}(\text{dach})(\text{dGMP})]$  with release of a chloride ion.

This  $2\text{e}^-$ ,  $2\text{H}^+$  oxidation process contrasts with the mechanism of autooxidation of a series of 6-oxopurines by  $[\text{Ru}^{\text{III}}(\text{NH}_3)_5]$  complex in basic media.<sup>5</sup> The  $\text{Ru}^{\text{III}}$  complex binds to N7 of inosine, leading to deprotonation of H8 and transfer of  $1\text{e}^-$  to  $\text{Ru}^{\text{III}}$ , and generates a radical at C8. This radical is attacked by water and undergoes a second  $1\text{e}^-$ ,  $1\text{H}^+$  oxidation to produce 8-ketonucleosides.

The formation of a cyclic 5',8-phosphodiester upon purine oxidation is a novel finding, although it is related to the observation of cyclic ethers formed in guanosine oxidation by nucleophilic attack of the 5'-hydroxyl at C8.<sup>17</sup> In the case of cyclic guanosine ethers, the product is stable toward further hydrolysis, while the cyclic phosphodiester obtained from  $\text{Pt}^{\text{IV}}$  oxidation of dGMP hydrolyzes over the course of several hours. The instability of the cyclic phosphodiester, compared to a 3',5'-phosphodiester linkage in DNA, could be due to ring strain in the nine-membered ring as well as the greater leaving group ability of 8-hydroxyguanine, which may be similar to a phenolate.

That a phosphate oxygen serves as the nucleophile suggests that the ring strain cannot be terribly high, since the high concentration of solvent would otherwise compete. If  $\text{H}_2\text{O}$  were the attacking nucleophile, 8-oxo-dGMP would be formed directly at this stage, and use of  $\text{H}_2^{18}\text{O}$  would lead to incorporation of the isotopically labeled oxygen at C8 of the base. In fact, careful analysis of the isotope ratios in the base-containing fragments (e.g.,  $m/z = 168$ ) from the ESI-MS/MS study of 8-oxo-dGMP formed in  $\text{H}_2^{18}\text{O}$  indicate that about 1% of the product derives from direct attack of water on the platinated intermediate rather than phosphodiester hydrolysis. This indicates that the intramolecular phosphate oxyanion is by far the best available nucleophile for the reaction of the mononucleotide. On the other hand, it is not known if a phosphodiester anion could play this role during  $\text{Pt}^{\text{IV}}$  oxidation of double-stranded DNA due to conformational restraints and the reduced nucleophilicity of a phosphodiester anion. However, other nucleophiles may be associated with duplex DNA in the cellular milieu, including polyamines and proteins containing nucleophilic side chains. For those cases where the  $\text{Pt}^{\text{IV}}$  complex has a sufficient intracellular concentration and lifetime, these studies suggest that  $\text{Pt}^{\text{IV}}$  oxidation of guanine in DNA could potentially be responsible for both mutagenic lesions such as 8-oxo-dG as well as formation of adducts or DNA–protein cross-links.

In summary, we have demonstrated that  $[\text{Pt}^{\text{IV}}\text{Cl}_4(\text{dach})]$  binds to N7 of guanine followed by an inner-sphere, two-electron redox reaction to form a novel intermediate, 8-hydroxyguanosine cyclic 5',8-(hydrogen phosphate), that slowly hydrolyzes to 8-oxo-dGMP. The biological implications of this mechanism and its applicability to dG in oligomers are currently under investigation.

## Experimental Section

**Materials.** [Pt<sup>IV</sup>Cl<sub>4</sub>(dach)] (tetraplatin) was obtained from the National Cancer Institute, Drug Synthesis and Chemistry Branch, Developmental Therapeutics Program, Division of Cancer Treatment. 8-oxo-dGMP was a gift from Professor Wallace at the University of Vermont.

**Reaction of [Pt<sup>IV</sup>Cl<sub>4</sub>(dach)] with dGMP.** Buffers were not used in order to avoid complications arising from buffer coordination to platinum.<sup>21</sup> Stock solutions (11 mM) of [Pt<sup>IV</sup>Cl<sub>4</sub>(dach)] was prepared by dissolving 11  $\mu$ mol of the Pt<sup>IV</sup> compound in 1 mL of H<sub>2</sub>O in an amber vial. The solubility of [Pt<sup>IV</sup>Cl<sub>4</sub>(dach)] is low, so several heating (maximum 50 °C) and vortexing cycles over 5 or 6 h were necessary for complete dissolution. After the Pt<sup>IV</sup> compound was dissolved, an appropriate amount of dGMP stock solution (100 mM) was added to give the desired final concentration. The pH of the solution was adjusted to pH 8.6 with 0.1 M NaOH. The time when the pH was adjusted to pH 8.6 was recorded as the beginning of the reaction. All the samples for NMR analysis were prepared in D<sub>2</sub>O (>98%). Most reaction solutions were filtered through a syringe-end filter disk (Gelman Acrodisc 0.45  $\mu$ m pore size) before HPLC and NMR analysis.

**Preparation of [Pt<sup>II</sup>Cl(dach)(dGMP)].** For reference purposes, [Pt<sup>II</sup>-Cl(dach)(dGMP)] was prepared by dissolving an appropriate amount of dGMP to give a final concentration of 1 mM dGMP in the 1 mM [Pt<sup>II</sup>Cl<sub>2</sub>(dach)]. It is noted that [Pt<sup>II</sup>(dach)(dGMP)<sub>2</sub>] was not produced even in the presence of excess (100-fold) dGMP for up to 3 days. [Pt<sup>II</sup>-Cl<sub>2</sub>(dach)] was obtained by reducing [Pt<sup>IV</sup>Cl<sub>4</sub>(dach)] with a 10-fold excess of ascorbic acid.<sup>22</sup> The reaction was allowed to proceed for 2 h, after which time a bright yellow-orange powder was obtained: IR (3267, 3190, 3066, 2936, 2863, 1564 cm<sup>-1</sup>).

**pH and Chloride Concentration.** pH and chloride concentration were measured with pH and chloride (Orion Model 94-17B) electrodes, respectively, connected to a pH meter (Orion Research 960).

**HPLC.** HPLC measurements were performed on either a Waters or a Beckman liquid chromatograph equipped with a diode-array detector. Isocratic (1 mL/min) conditions with a Waters symmetry shield RP18 (5  $\mu$ m, 4.6 mm  $\times$  250 mm) column and solvent consisting of 95% triethylammonium acetate (50 mM, pH 7.0) and 5% methanol were the best for the elution of **I** and [Pt<sup>II</sup>Cl(dach)(dGMP)] at reasonable retention times (10.9 and 7.5 min, respectively). Isocratic conditions (1 mL/min) with a RESTEK Ultra IBD (5  $\mu$ m, 4.6 mm  $\times$  250 mm) column and solvent consisting of 98% ammonium acetate (20 mM, pH 5.8) and 2% acetonitrile gave the best resolution for the components in the reaction mixture (Figure 7). However, one drawback for these

conditions was that the retention times of **I** and [Pt<sup>II</sup>Cl(dach)(dGMP)] were long (>40 min).

**NMR.** NMR spectra were recorded on a Bruker NMR spectrometer equipped with a broad-band inverse tunable probe operating at 400.13 MHz for <sup>1</sup>H and 161.97 MHz for <sup>31</sup>P. Chemical shifts for <sup>1</sup>H and <sup>31</sup>P are reported relative to tetramethylsilane (TMS) and 85% H<sub>3</sub>PO<sub>4</sub>, respectively, each at 0.00 ppm. Samples were prepared in D<sub>2</sub>O and the residual water signal was further suppressed by the watergate pulse sequence.<sup>23</sup> Time-course experiments were performed at 37 °C by recording spectra at 1 h intervals by use of a multiple acquisition program (total acquisition time + delay between experiments = 1 h) with 256 scans for <sup>1</sup>H or 1000 scans for <sup>31</sup>P with broad-band <sup>1</sup>H decoupling.

**ESI-MS.** Labeled and unlabeled samples were analyzed by positive-ion electrospray ionization (ESI) on a Micromass Quattro II tandem mass spectrometer equipped with a Zspray API source. Samples were dissolved in acetonitrile and water (1:1) and introduced via infusion at a flow rate of 0.30 mL/h. The source and desolvation temperatures were 80 and 120 °C, respectively. The capillary voltage was set to 3.1 kV, sampling cone voltage to 58 V, and the extractor cone to 3 V. The collision energy was set to 14 eV. Argon, used as a collision gas for the CID experiments, was adjusted to a pressure of 1.7  $\times$  10<sup>-4</sup> mBar. In a representative experiment, MS-1 was set to the mass for the nucleotide and the precursor ion was subjected to CID in the static quadrupole. The resulting spectrum of the products recorded by scanning the second scanning analyzer (MS-2) between 50 and 370 Da. The scan duration and the interscan delay time were 3.0 and 0.1 s, respectively. The instrument was operated and data were accumulated with Micromass Masslynx software (version 3.2).

**Acknowledgment.** This work was supported by the National Institutes of Health (1 R15 CA82145-01), the Petroleum Research Fund administered by the American Chemical Society (37874-B3), the Vermont Genetics Network through NIH (1 P20 RR16462 from the BRIN program of the National Center for Research Resources), and the National Science Foundation (0137716 to C.J.B.) including an ROA supplement for partial funding of S.C.'s sabbatical at the University of Utah. The mass spectrometer used in this study was purchased with funds from the NSF (9807669) and the University of Utah Institutional Funds Committee. We thank Professor Roger Sandwick for helping us with <sup>31</sup>P NMR spectroscopy.

JA038334M

(21) (a) Lempers, E. L. M.; Bloemink, M. J.; Reedijk, J. *Inorg. Chem.* **1991**, *30*, 201–206. (b) Barnham, K. J.; Guo, Z.; Sadler, P. J. *J. Chem. Soc., Dalton Trans.* **1996**, 2867–2876.

(22) Blatter, E. E.; Vollano, J. F.; Krishnan, B. S.; Dabrowiak, J. C. *Biochemistry* **1984**, *23*, 4817–4820.

(23) Trimble, L. A.; Bernstein, M. A. *J. Magn. Reson., Ser. B.* **1994**, *105*, 67–72.